

Current understanding of tokamak plasma eruption control and the consequences for ITER

Joe Allen, JOA509

19th May 2016

1 Abstract

Here will lie the abstract

2 Background

Since their experimental observation over thirty years ago[1], edge localised modes (ELMs) have attracted a large amount of research interest. Toroidal magnetic field devices looking to maximise power production must operate in the high confinement regime (H-mode), in which the central plasma density profile is raised up on a pedestal, providing enhanced confinement.[2] This elevation is caused by a steep pressure gradient in the separatrix (the boundary between open and closed field lines at the edge of the plasma). Due to the unstable nature of this gradient, ELMs periodically disrupt the edge plasma, causing energy and particle losses; ELMs are a type of magnetohydrodynamic (MHD) instability.[3]

In H-mode, type I ELMs are initiated when the pressure increases such that it reaches the ideal peeling-ballooning (PB) stability boundary, the manner of this cyclic process is shown in figure 1. This model was proposed in 2002[4] and has since been developed and corroborated with experimental evidence.[5] More specifically, the high edge pressure gradient drives a large bootstrap current in the region which in turn produces $n \sim 3-30$ modes[6] which lead to eruptions from the plasma edge. The edge plasma rapidly collapses as the PB boundary is approached; this collapse is due to the non-linear growth of MHD instabilities [7] that is observed when the edge pressure and current values near the two stability limits.

Table 1: The different instability modes resulting from combinations of pedestal pressure, p_{ped} , and current J_{ped} . [8]

p_{ped}	J_{ped}	Mode
High	Low	Ballooning
Low	High	Peeling
High	High	Peeling-ballooning

Increasing collisionality reduces edge current densities

Level of plasma shaping has a drastic effect on the size of the stable region below the PB limit, which can be seen in figure 3, an example being increased triangularity extends the stable region to encompass higher edge pressure and current values [8].

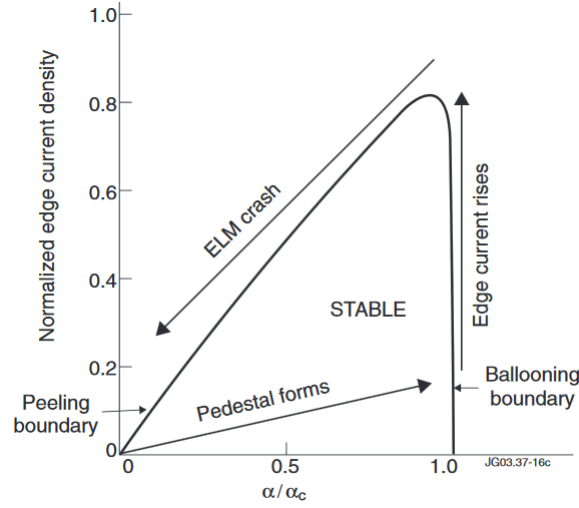


Figure 1: Pressure-current pathway followed throughout an ELM cycle[9]. An ELM is initiated when the peeling stability boundary is passed in the top right corner, returning the edge to a low pressure, low current state in the bottom left corner. The edge pressure is then built up quite rapidly to the ballooning limit by heating, compared to the edge current which increases more slowly, on a resistive timescale, until the crash. The edge pressure rests at the ballooning limit until the current increases across the peeling limit. Normalised edge pressure is on the x -axis.

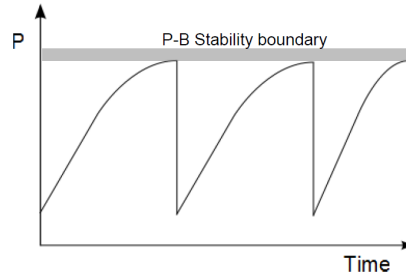


Figure 2: H-mode pressure cycle up to the peeling-ballooning limit which triggers ELMs [10].

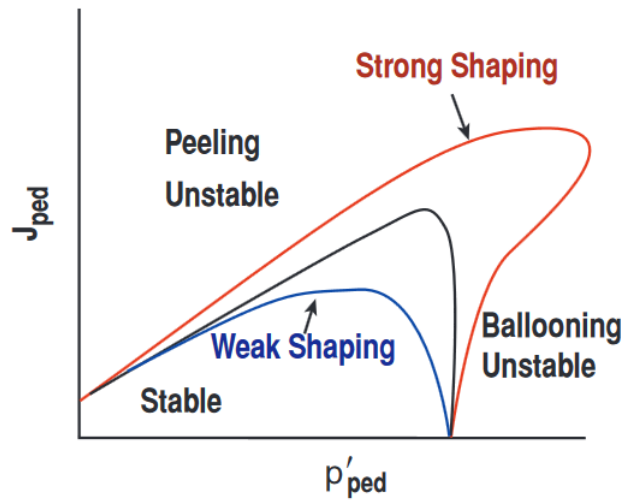


Figure 3: Differing peeling-ballooning stability boundaries for varying degrees of plasma shaping [11].

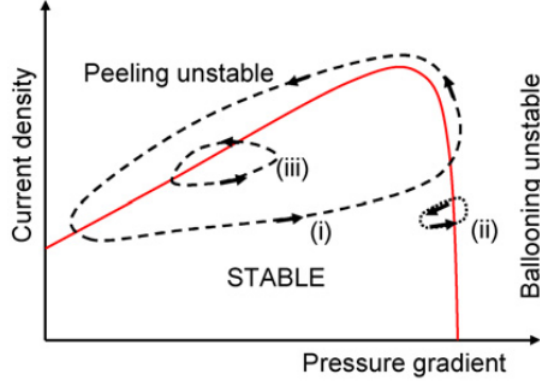


Figure 4: (i) Qualitative ELM cycle pathways: peeling-ballooning limit breached causes a large type I ELM; (ii) ballooning limit breached, produces either small ELMs or none at all; (iii) peeling limit breached causes a small ELM [12].

Current understanding is that ELMs of different magnitudes are produced depending on which stability boundary is infringed, visualised in figure 4. The possibility of no ELMs being produced in case (ii) is a result of the fact that the enhanced transport due to the breach reduces the edge pressure gradient which prevents an eruption [12].

Despite the many negative effects of ELMs on reactor lifetime, they do drive some positive processes such as enhanced transport which reduces impurity fraction in the bulk plasma. As a result of this, a controlled amount of low power ELMs may be desired to keep the core clean and give the ability to control the plasma density.[13] The positive impact of this impurity removal is greater than the resulting drop in fusion performance due to loss of energy confinement.[14]

Edge-plasma eruptions can easily be viewed by measuring the corresponding peak in H_α emission at the eruption position.[13]

”Observations about ELMs:

1. They tend to limit energy confinement
2. they provide density control and limit the buildup of impurities in H-mode
3. they broaden the scrape-off layer density profile and modulate ICRH antenna coupling
4. they produce large heat pulses on the plasma facing components
5. they increase sputtering of first-wall materials

”Type 3 ELMs are observed when the power crossing the separatrix is just above the H-mode power threshold, and may result from resistive instabilities, since they occur at pressure gradients well below the ideal limit and can be stabilized by increasing the edge electron temperature”[13]

Hill 1997[13] says it is not understood why ELMs produce a large heat pulse at the inner divertor target than at the outer plates (in single-null divertors)

What changes ELM frequency: ”The critical pressure gradient for the destabilization of the ideal ballooning mode [6] depends on the local flux-surface averaged magnetic shear, S , and the safety factor, q , which Gohil evaluated at the 95% flux surface in his study (S_{95}/q_{295}). Thus, anything which increases the rate that the pressure builds up reduces the time required to hit the stability limit and increases the ELM frequency, while anything that raises the limit,

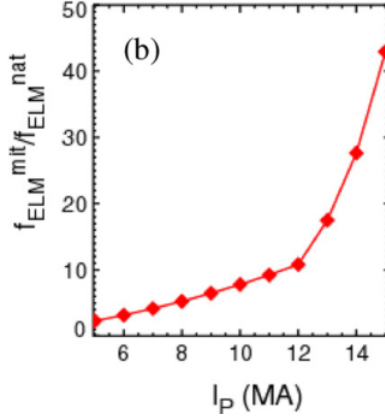


Figure 5: The required ratio of mitigated to natural ELM frequency to safeguard the performance for both a single discharge, keeping W impurity levels sufficiently low, and for the long term of ITER [18].

such as increasing the current (lowers q_{95}) or triangularity (increases S), increases the time required to hit the stability limit and reduces the ELM frequency.”[13]

Several tokamaks have corroborated the scaling of ELM frequency given in equation 1 [15][16], showing that it may be possible to externally decrease the time between ELMs in order to reduce their magnitude. P_{SOL} is essentially fixed for a given machine and is estimated to be approximately 100 MW in ITER.[17]

$$f_{ELM}\Delta W_{ELM} = 0.2 - 0.4P_{SOL} \quad (1)$$

Edge collisionality has an important role in the effectiveness of ELM control, when using RMP coils it can be the deciding factor between ELM suppression and mitigation [18]. Suppression is complete removal of ELMs, whereas mitigation is when their frequency is increased (causing a corresponding decrease in power due to equation 1).

3 Problems for ITER

ELMs R (mostly) Bad [14]

A limit has been set on the maximum power fluxes allowed onto the PFCs, specifically half that which would melt these components.[19] Natural ELM frequency for ITER will be about 1 Hz and the resultant power load on the plasma facing components (PFCs) will cause them and the tungsten (W) divertor plates to melt[20]. ITER will not be able to stand even one ELM of this magnitude and so it must operate in a completely ELM-mitigated regime[10]. Current research tokamaks are able to derive the parameters for ELM suppression and mitigation at regular operating power. ITER is simply too powerful and thus does not have this luxury.

ITER will be able to tolerate ELM energies of under 1 MJ per eruption; given that a single ELM can release a small fraction of the entire plasma energy, estimated to be up to around 20% of the pedestal plasma energy[21]. Thus, a natural type I ELM in ITER could release 20 MJ in 500 μs [10], which is an unfeasibly high heat flux for the device. ITER is designed to operate at $I_p = 15$ MA and $Q_{DT} = 10$; however, if it lacks the necessary ability to control ELMs the divertor and PFCs will start to degrade faster than desirable at plasma currents of 6 – 9 MA.[8] Extended operation in the designed scenario would then not be possible.

Predictions have been drawn from analysis of data from current machines as to the maximum ELM energy flux impacting the divertor which does not significantly impact its lifetime: for the design scenario above ($I_p = 15$ MA, $Q_{DT} = 10$) this is approximately 0.5 MJ m^{-2} [22]. ITER is expected to have a natural ELM frequency of around 1 Hz[10] and there are estimated to be between 500 – 1000 ELMs per shot in the $Q_{DT} = 10$ scenario. If each ELM in this operating scenario causes a degradation of $0.1\mu\text{m}$ in an area of the W divertor, the capability of ITER will be reduced to less than thirty days of operation or a maximum of 100 shots[8] (assuming four discharges per day). With a cost exceeding 100 M [23] and an long period of enforced downtime during replacement, the collaboration cannot afford to render the divertor useless so quickly. 100.

Another import factor is the ELM divertor footprint - the area of energy deposition on the divertor plates - which has been shown to decrease with decreasing ΔW_{ELM} [24]. While being beneficial for uncontrolled natural ELMs this somewhat reduces the effectiveness of increasing f_{ELM} , regarding equation 1, as the heat flux incident on the divertor will not fall indefinitely with decreasing ΔW_{ELM} due to the divertor footprint becoming very small.

The maximum allowed energy flux per ELM of 0.5 MJ m^{-2} can be translated into a maximum loss of energy by the plasma per ELM which, when calculated gives $\Delta W_{ELM} = 0.66 \text{ MJ}$ [25]. This limit requires a thirty fold decrease in ELM energy from the natural ΔW_{ELM} of 20 MJ.

include some figures from Kirk’s talk showing the varying requirements on ELM frequency enforced by these different factors (PFC health, impurity levels etc.)

There is a limit on the minimum ELM frequency necessary for ITER’s operation due to the need to remove impurities (page5/6)[19], unless other methods of enhancing transport can be utilised.

4 Current methods for ELM control

4.1 Resonant Magnetic Perturbations (RMPs)

RMP ELM control seeks to influence the edge plasma so as to hold it below the PB stability limit throughout the discharge. If the edge pressure can be maintained just under this limit type I ELMs will not be triggered; this is very beneficial to the overall fusion performance of the machine as the core plasma will a sufficiently high pressure. If the transport rate in the edge transport barrier (ETB) can be augmented through external influence the plasma pressure can be made to level off below the critical PB stability boundary.

Plasma density and confinement are reduced by around 10% by the use of RMP coils [8]; nevertheless, researchers using ASDEX Upgrade (AUG) saw a factor 6 reduction in core plasma energy loss in ELM-mitigated shots with $n_{RMP} = 2$ toroidal edge perturbations [26]. Again on AUG, pellet injection was used to combat the density reduction in ELM mitigated regime and also to bring the edge density above the threshold level necessary to reach said ELM mitigated regime [27]. There appears to exist a minimum edge plasma density below which ELM mitigation will not occur [26], hence pellet injection will need to be used in tandem with RMP control in ITER in order to keep the edge density above this threshold throughout the duration of a shot.

A mechanism for

DIID-D has been used to investigate ELM suppression in plasmas with similar shapes and collisionalities to ITER [28, 29], with suppression at collisionalities $\nu_c^* < 0.35$ but only mitigation above that. Experiments on MAST[30] using $n_{RMP} = 4$ and 6 have achieved mitigation,

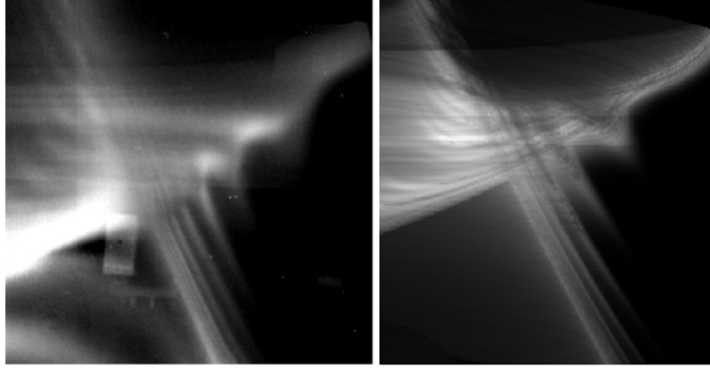


Figure 6: Camera image of $n_{RMP} = 6$ X-point lobes on MAST (left), ERGOS simulation for comparison (right) [35].

increasing f_{ELM} eightfold. KSTAR has seen, with $n_{RMP} = 1$, complete suppression of ELMs and also two distinct stages after RMP activation. First the plasma energy, toroidal rotation and density decrease by a small factor while the ELMs are being suppressed. Secondly, when ELMs are fully suppressed, these quantities plateau [31]. At AUG, similar discoveries have been made using $n_{RMP} = 2$ [26, 32] and, perhaps most importantly, strong mitigation was observed on JET under operation with an ITER-like wall [33].

ITER’s tungsten divertor introduces further requirements on ELM control[10] W build up in the plasma core could cause catastrophic energy losses; hence, additional methods to provide enhanced transport will need to be implemented, else low power ELMs must be allowed to occur to provide this enhancement. ELMs, however, are the main source of divertor impurities in the main plasma, so their suppression could itself be sufficient to bring core levels of W below the required threshold. Experiments on AUG found that in a type I ELM-mitigated regime the fraction of W in the plasma is lower by a factor of 2 compared to in unmitigated regimes [26].

The magnitude of field applied by RMP coils is $10^{-4} \sim 10^{-3}$ T [34]. These relatively tiny perturbations disrupt the toroidal symmetry of the magnetic field, making it 3D rather than 2D. Field line paths become direction specific (clockwise path is different from the anti-clockwise path) and the edge flux surfaces are no longer smooth but instead exhibit lobe structures, especially in the X-point region. Visualisation of these lobes can be seen in figure 6, showing very good overlap between the simulated and experimental data.

The X-point lobe patterns’ radial length scales linearly with the magnitude of the applied RMP. They develop more complexity and size with increasing perturbation mode number [35]. More specifically, their size increases radially yet they have a smaller poloidal spread for increasing n_{RMP} [36]. These lobes pose a danger for the divertor plates: now the heat flux is 3D, their erosion will not be isotropic over the plates, causing roughening of the surface which will further enhance the heat load disparity. This separatrix splitting was first observed on MAST [37] and soon after on DIII-D [38].

4.2 Pellet Injection

ELM magnitude scales as $f_{ELM} \cdot \Delta W_{ELM} \sim \text{constant}$ [10, 15, 16], so influencing factors which decrease the time between ELMs will consequently decrease their power. Sufficiently increasing f_{ELM} has the benefit of ensuring that no one single ELM will cause critical damage to the PFCs or the divertor; however, high repetition rate thermal cycling of of these first layer components may have severe long term impacts. Much research is under way to ascertain more precisely the

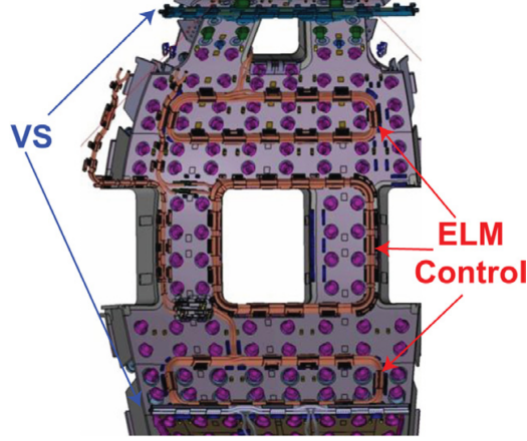


Figure 7: RMP (ELM control) and vertical stability (VS) coil layout on one ninth of the ITER outboard vessel wall [8].

thermal cycling tolerances of these components. Large networks of cracks can form in tungsten tiles after repeated exposure to type I ELM-like heat fluxes [39], which could be extremely detrimental to the extended operation of ITER.

As discussed in section 3, the ELM deposition area on the divertor scales with ELM energy. In ITER's testing phase the full extent of this relationship must be established in order to gauge how high it is beneficial to raise f_{ELM} by pellet pacing (or another triggering method). If said relationship was found to be very firm it will make these triggering methods redundant for ELM damage reduction [8].

4.3 Vertical Kicks

Fractional shifts in the vertical position of the plasma, $\sim 1 - 3\%$ of the minor radius[10], executed rapidly augment the edge current to attempt to mitigate ELMs.[40]

ASDEX-U trialled the first usage of pellets to trigger ELMs in 2003.[41] Projectile pellets provoke type 1 ELMs when they penetrate into the pedestal.[10]

4.4 Evidence for these methods in practice

DIII-D experiment showing complete ELM suppression (DIII-D geometry is similar to ITER's)[42]

References on Slide 45 of A. Kirk's talk about ELM (I) suppression at low collisionality. *****What exactly is collisionality, how is it measured and how is it externally influenced?***** Lowering collisionality, ν^* , causes the pressure cycle to retreat from the unstable peeling-ballooning region and thus leads to complete type I ELM suppression.[28]

4.5 How these methods will work on ITER

ITER will utilise at least two major ELM control systems, RMP coils and pellet injectors [43]. Figure 7 shows the planned positions of the ELM control coils in ITER.

In order to counteract the uneven divertor heat loads due to the flux surface lobes produced by the RMP coils, the perturbations will be rotated toroidally above 1 Hz [22] so as to smear out the deleterious effects over the whole divertor. Alternatively the toroidal mode number

of the perturbation could be cycled. Different edge perturbations investigated on MAST, $n_{RMP} = 2, 3, 4$ and 6, found that the footprint at the divertor changed for each value of n_{RMP} [36]. The problem with this partial solution is that cycling could damage the RMP coils in the long term [10]. This is very undesirable as they are within the first vacuum wall and so cannot be replaced.

Currently, ITER is expected to use $n_{RMP} = 3$ and 4 [36]. A decision made after the success on DIII-D of complete suppression, in similar conditions to the ITER baseline scenario, using $n_{RMP} = 3$ in 2008 [28, 44]. The understanding of this suppression was more recently advanced by Wade *et al.* [45]. The group found that it is the alignment of the $n = 3$ rational surface with zero perpendicular electron velocity ($\omega_{\perp e} = 0$) and the pedestal peak that is critical in achieving suppression. Regarding the requirement $\omega_{\perp e} = 0$, it was found necessary to apply neutral beam injection (NBI) with the plasma rotation, as anti-rotation application does not produce a $\omega_{\perp e} = 0$ region, preventing ELM suppression altogether [45].

Snyder *et al.* have proposed a mechanism for RMP induced suppression [46], in which a stochastic ¹ region or layer of resonant magnetic islands form due to the RMP penetration of the edge plasma. This enhances the rate of edge transport which ensures the edge pressure and current density remain below the peeling-ballooning boundary.

Edge safety factor, q_{95} - safety factor at 95% poloidal flux, imposes strict boundaries on suppression on DIII-D. ELM suppression is only seen for $3.32 < q_{95} < 3.67$ [44], which poses issues as the expected value is around $q_{95} = 3$ in the default ITER scenario [47]. This "q-window" in which suppression occurs is less wide for ITER similar shaped (ISS) plasmas than for plasma shapes with lower triangularity [28].

The explanation [46] of RMP suppression also provides potential answer for the existence of these "q-windows".

Plasma response to RMP activation is discussed in [48].

Vertical stability coils may be implemented as a fall back ELM control method [19]. VS coils were already included into the design, just not initially for ELM triggering.

5 Necessary future work

Before the first plasma run in ITER, it must be able to operate in a regime with strictly controlled ELMs in order to ensure a reasonable lifetime of the machine. More work is required to build a stronger physical basis of suppression and mitigation in ITER-like scenarios, building from DIII-D [28, 29] and JET [33] experiments, such that more realistic extrapolations can be drawn regarding the potential success of these control techniques on ITER.

Alongside the development of the optimal RMP mode to apply in ITER's different regimes, there must be continual assessment of the projected lifetimes of the ELM control coils. Provisions need to be made for the worst case scenario in which several coils fail quickly: a protocol of which perturbations are conducted depending on the arrangement of the remaining coils.

Quiescent H-mode (QH-mode) retains the benefits of the central pedestal without the cyclic energy losses by ELMs, which are damaging to both fusion performance and the device's components. It has been attained on several tokamaks; namely DIII-D, JET and ASDEX-U [49, 50], and is a potentially promising operating regime for ITER if enough prior research and solid extrapolation can be performed.

¹having a random probability distribution

5.1 I-Mode

The I-mode is an operating regime that combines the desirable elements of H- and L-mode [51] and has automatic ELM suppression [52]. It is more easily available to higher-field machines and has been investigated most considerably on Alcator C-Mod. Core impurity levels are lowered in I-mode as it lacks an edge particle transport barrier, while retaining the edge energy transport barrier. Hence, I-mode can be distinguished by observing an H-mode like temperature pedestal along with an L-mode like density profile.[51]

References

- [1] M. Keilhacker et al. “Confinement studies in L and H-type Asdex discharges”. In: *Plasma Physics and Controlled Fusion* 25.1A (1984), pp. 49–63.
- [2] F. Wagner. “A quarter-century of H-mode studies”. In: *Plasma Physics and Controlled Fusion* 49.12B (2007), pp. 1–33.
- [3] H Zohm. “Edge localized modes (ELMs)”. In: *Plasma Physics and Controlled Fusion* 38.2 (1996), pp. 105–128.
- [4] P. B. Snyder et al. “Edge localized modes and the pedestal: A model based on coupled peeling-ballooning modes”. In: *Physics of Plasmas* 9.5 (2002), pp. 2037–2043.
- [5] H. R. Wilson et al. “Numerical studies of edge localized instabilities in tokamaks”. In: *Physics of Plasmas* 9.4 (2002), p. 1277.
- [6] P.B. Snyder et al. “Pedestal stability comparison and ITER pedestal prediction”. In: *Nuclear Fusion* 49.8 (2009), p. 085035.
- [7] H. R. Wilson and S. C. Cowley. “Theory for explosive ideal magnetohydrodynamic instabilities in plasmas”. In: *Physical Review Letters* 92.17 (2004), pp. 175006–1.
- [8] P.T. Lang et al. “ELM control strategies and tools: status and potential for ITER”. In: *Nuclear Fusion* 53.4 (2013), p. 043004.
- [9] C P Perez et al. “Washboard modes as ELM-related events in JET”. In: *Plasma Physics and Controlled Fusion* 46.1 (2004), pp. 61–87.
- [10] *Controlling plasma eruptions in tokamaks*. Fusion Frontiers Lectures. Kirk, A. 2016.
- [11] P B Snyder et al. “Characterization of peelingballooning stability limits on the pedestal”. In: *Plasma Physics and Controlled Fusion* 46.5A (2004), A131–A141.
- [12] H. R. Wilson et al. “Magneto-hydrodynamic stability of the H-mode transport barrier as a model for edge localized modes: an overview”. In: *Plasma Physics and Controlled Fusion* 48 (2006), A71–A84.
- [13] D.N. Hill. “A review of ELMs in divertor tokamaks”. In: *Journal of Nuclear Materials* 241-243 (1997), pp. 182–198.
- [14] J. W. Connor et al. “Edge Localised Modes (ELMs): Experiments and Theory”. In: *AIP Conference Proceedings* 1013 (2008), pp. 174–190.
- [15] A. W. Leonard et al. “Impact of ELMs on the ITER divertor”. In: *Journal of Nuclear Materials* 266 (1999), pp. 109–117.

- [16] A. Loarte et al. “Characteristics and scaling of energy and particle losses during Type I ELMs in JET H-modes”. In: *Plasma Physics and Controlled Fusion* 44.9 (2002), pp. 1815–1844.
- [17] T. Eich et al. “Scaling of the tokamak near the scrape-off layer H-mode power width and implications for ITER”. In: *Nuclear Fusion* 53.9 (2013), p. 093031.
- [18] A. Kirk et al. “Understanding the effect resonant magnetic perturbations have on ELMs”. In: *Physical Review Letters* 108.25 (2013), p. 32. arXiv: 1306.6841.
- [19] A. Loarte et al. “Progress on the application of ELM control schemes to ITER scenarios from the non-active phase to DT operation”. In: *Nuclear Fusion* 54.3 (2014), p. 033007.
- [20] G Federici, a Loarte and G Strohmayer. “Assessment of erosion of the ITER divertor targets during type I ELMs”. In: *Plasma Physics and Controlled Fusion* 45.9 (2003), pp. 1523–1547.
- [21] A Loarte et al. “Characteristics of type I ELM energy and particle losses in existing devices and their extrapolation to ITER”. In: *Plasma Physics and Controlled Fusion* 45.9 (2003), pp. 1549–1569.
- [22] A. Loarte. *Plan for ELM Mitigation in ITER. Technical Report No. 1*. Tech. rep. ITER, 2013.
- [23] *THE WEST* PROJECT: preparing ITER full tungsten divertor operation*. ORNL PMIF-PFC. Tsitrone, E. 2013.
- [24] T. Eich et al. “Type-I ELM power deposition profile width and temporal shape in JET”. In: *Journal of Nuclear Materials* 415.1 SUPPL (2011), S856–S859.
- [25] *23rd IAEA Fusion Energy Conference*. Loarte, A. 11-16 October 2010, Daejeon, Republic of Korea. www-naweb.iaea.org/napc/physics/FEC/FEC2010/html/index.htm.
- [26] W. Suttrop et al. “First observation of edge localized modes mitigation with resonant and nonresonant magnetic perturbations in ASDEX upgrade”. In: *Physical Review Letters* 106.22 (2011), pp. 1–4.
- [27] P.T. Lang et al. “High-density H-mode operation by pellet injection and ELM mitigation with the new active in-vessel saddle coils in ASDEX Upgrade”. In: *Nuclear Fusion* 52.2 (2012), p. 023017.
- [28] T E Evans et al. “RMP ELM suppression in DIII-D plasmas with ITER similar shapes and collisionalities”. In: *Nuclear Fusion* 48.2 (2008), p. 10.
- [29] M J Lanctot et al. “Sustained suppression of type-I edge-localized modes with dominantly $n=2$ magnetic fields in DIII-D”. In: *Nuclear Fusion* 53.8 (2013), p. 9.
- [30] A Kirk et al. “Understanding edge-localized mode mitigation by resonant magnetic perturbations on MAST”. In: *Nuclear Fusion* 53.4 (2013), p. 043007. arXiv: 1305.3723.
- [31] Jong-Gu Kwak et al. “An overview of KSTAR results”. In: *Nuclear Fusion* 53.10 (2013), p. 104005.
- [32] R Fischer et al. “Spatiotemporal response of plasma edge density and temperature to non-axisymmetric magnetic perturbations at ASDEX Upgrade”. In: *Plasma Physics and Controlled Fusion* 54.11 (2012), p. 115008.
- [33] Y Liang et al. “Mitigation of type-I ELMs with $n=2$ fields on JET with ITER-like wall”. In: *Nuclear Fusion* 53.7 (2013), p. 9.

- [34] T. E. Evans. “Resonant magnetic perturbations of edge-plasmas in toroidal confinement devices”. In: *Plasma Physics and Controlled Fusion* 57.12 (2015), p. 123001.
- [35] J.R. Harrison et al. “Characteristics of X-point lobe structures in single-null discharges on MAST”. In: *Nuclear Fusion* 54.6 (2014), p. 064015.
- [36] I.T. Chapman et al. “Assessing the merits of resonant magnetic perturbations with different toroidal mode numbers for controlling edge localised modes”. In: *Nuclear Fusion* 54.12 (2014), p. 123003.
- [37] A. Kirk et al. “Observation of lobes near the X point in resonant magnetic perturbation experiments on MAST”. In: *Physical Review Letters* 108.25 (2012), pp. 1–4.
- [38] M.W. Shafer et al. “Experimental imaging of separatrix splitting on DIII-D”. In: *Nuclear Fusion* 52.12 (2012), p. 122001.
- [39] J. Linke et al. “Performance of different tungsten grades under transient thermal loads”. In: *Nuclear Fusion* 51.7 (2011), p. 073017.
- [40] E. de la Luna et al. “Understanding the physics of ELM pacing via vertical kicks in JET in view of ITER”. In: *Nuclear Fusion* 56.2 (2016), p. 026001.
- [41] P T Lang et al. “ELM frequency control by continuous small pellet injection in ASDEX Upgrade”. In: *Nuclear Fusion* 43.10 (2003), pp. 1110–1120.
- [42] S Mordijck et al. “Comparison of resonant magnetic perturbation-induced particle transport changes in H-mode (DIII-D) and L-mode (MAST)”. In: *Plasma Physics and Controlled Fusion* 53.12 (2011), p. 122001.
- [43] A. Loarte. “23rd IAEA Fusion Energy Conference, 1116 October 2010, Daejeon, Republic of Korea, Book of Abstracts”. In: October. 2010, pp. 545–546.
- [44] M. E. Fenstermacher et al. “Effect of island overlap on edge localized mode suppression by resonant magnetic perturbations in DIII-D”. In: *Physics of Plasmas* 15.5 (2008).
- [45] M. R. Wade et al. “Advances in the physics understanding of ELM suppression using resonant magnetic perturbations in DIII-D”. In: *Nuclear Fusion* 55.2 (2015), p. 23002.
- [46] P. B. Snyder et al. “The EPED pedestal model and edge localized mode-suppressed regimes: Studies of quiescent H-mode and development of a model for edge localized mode suppression via resonant magnetic perturbations”. In: *Physics of Plasmas* 19.5 (2012).
- [47] C Gormezano et al. “Chapter 6: Steady state operation”. In: *Nuclear Fusion* 47 (2007), S285–S336.
- [48] F.L. Waelbroeck. “Theory and observations of magnetic islands”. In: *Nuclear Fusion* 49.10 (2009), p. 104025.
- [49] K.H. Burrell et al. “Quiescent H-mode plasmas in the DIII-D tokamak”. In: *Plasma Physics and Controlled Fusion* 44.A (2002), pp. 253–263.
- [50] W Suttrop et al. “Studies of the Quiescent H-mode’ regime in ASDEX Upgrade and JET”. In: *Nuclear Fusion* 45.7 (2005), pp. 721–730.
- [51] D.G. Whyte et al. “I-mode: an H-mode energy confinement regime with L-mode particle transport in Alcator C-Mod”. In: *Nuclear Fusion* 50.10 (2010), p. 105005.
- [52] E.S. Marmar et al. “Alcator C-Mod: research in support of ITER and steps beyond”. In: *Nuclear Fusion* 55.10 (2015), p. 104020.